THE JOURNAL OF BIOLOGICAL CHEMISTRY
Vol. 279, No. 27, Issue of July 2, pp. 28553–28563, 2004

Printed in U.S.A.

Two Discontinuous Segments in the Carboxyl Terminus Are Required for Membrane Targeting of the Rat γ-Aminobutyric Acid Transporter-1 (GAT1)*

Received for publication, July 9, 2003, and in revised form, March 16, 2004
Published, JBC Papers in Press, April 8, 2004, DOI 10.1074/jbc.M307325200

Hesso Farhan, Vladimir M. Korkhov, Verena Paulitschke, Mario M. Dorostkar, Petra Scholze, Oliver Kudlacek, Michael Freissmuth‡, and Harald H. Sitte

From the Institute of Pharmacology, Medical University of Vienna, Währinger Str. 13a, A-1090 Vienna, Austria

Like all members of the Na^+/Cl^--dependent neurotransmitter transporter family, the rat γ-aminobutyric acid transporter-1 (GAT1) is sorted and targeted to specialized domains of the cell surface. Here we identify two discontinuous signals in the carboxyl terminus of GAT1 that cooperate to drive surface expression. This conclusion is based on the following observations. Upon deletion of the last 37 amino acids, the resulting GAT1-Δ37 remained trapped in the endoplasmic reticulum. The presence of 10 additional residues (GAT1-Δ27) sufficed to support the interaction with the coat protein complex II component Sec24D; surface expression of GAT1-Δ27 reached 50% of the wild type level. Additional extensions up to the position −3 (GAT1-Δ3) did not further enhance surface expression. Thus the last three amino acids (AYI) comprise a second distal signal. The sequence AYI is reminiscent of a type II PDZ-binding motif; accordingly substituting Glu for Ile abrogated the effect of this motif. Neither the AYI motif nor the last 10 residues rescued the protein from intracellular retention when grafted onto GAT1-Δ37 and GAT1-Δ32; the AYI motif was dispensable for targeting of GAT1 to the growth cone of differentiating PC12 cells. We therefore conclude that the two segments act in a hierarchical manner such that the proximal motif (^{569}VMI^{571}) supports endoplasmic reticulum export of the protein and the distal AYI motif places GAT1 under the control of the exocyst.

Neurotransmission at synaptic junctions in the central nervous system is terminated by reuptake of the neurotransmitter into the synaptic ends (1). This is achieved by neurotransmitter transporters. GABA[1] is the major inhibitory neurotransmitter in the brain. There are three GABA transporters, referred to as GAT1, GAT2, and GAT3, which all belong to the Na^+/Cl^--dependent neurotransmitter transporter family. Members of this family share several features including a characteristic topology, *i.e.* intracellular amino and the carboxyl termini and a hydrophobic core composed of 12 transmembrane-spanning segments that are presumed to be predominantly α-helical. In the brain, GAT1 is the most widely distributed isoform. The transporter is of obvious therapeutic relevance: increases in synaptic GABA reduces excitability and prevents excessive neuronal firing. This action provides a rationale for the use of tiagabine in the treatment of epilepsy (2).

In neurons, transporters must reach the presynaptic specialization. Thus, their biosynthetic pathway must also comprise mechanisms that afford the sorting and targeting to the axonal compartment and/or specific retention at perisynaptic sites (3). In addition, they undergo quality control in the endoplasmic reticulum (4) and posttranslational modification in the Golgi stacks. We recently demonstrated that neurotransmitter transporters such as GAT1 and the serotonin transporter form constitutive oligomers (5). If oligomerization of GAT1 is disrupted, the transporter is no longer expressed at the cell surface but is retained in the endoplasmic reticulum (6). However, while exit from the endoplasmic reticulum is contingent on the association of transporter homo-oligomers, oligomerization does not suffice, and additional sequence elements in the intracellular segments are required. In fact, if the entire carboxyl terminus is truncated, GAT1 is also retained (6). Perego *et al.* (7) showed that deletion of 36 amino acids from the carboxyl terminus of GAT1 did not affect membrane targeting and polarized sorting of the transporter in MDCK cells. The authors concluded that the major part of the GAT1 carboxyl terminus was dispensable for sorting the protein into the correct compartment. Thus, based on these results, we initially focused on the part of GAT1 adjacent to the last transmembrane segment to identify sequence elements that specify targeting to the plasma membrane. In the present work, we show that GAT1 mutants, which lack up to 29 amino acids of the carboxyl terminus, are retained within the cell. We uncovered two discontinuous signals, which act in a hierarchical manner. The proximal one (^{569}VMI^{571}) is responsible for sorting the protein into the correct compartment. The distal signal is comprised of the last three amino acids, which apparently fulfill the criteria of a type II PDZ interaction domain, and functions to accelerate membrane insertion.

EXPERIMENTAL PROCEDURES

Materials, Reagents, and Mutagenesis—ER Tracker Blue-White DPX, a fluorescent dye that specifically stains the endoplasmic reticulum, was from Molecular Probes (Leiden, The Netherlands). The sources of the other chemicals and reagents have been listed previously (6). Plasmids encoding amino-terminally tagged YFP-Sec24D (from rat) and various versions of Exo70 (from rat) were kind gifts from Drs. R.

* This work was supported by Austrian Science Foundation (FWF) Grants P15034 (to M. F.) and P14509 (to H. H. S.). The costs of publication of this article were defrayed in part by the payment of page charges. This article must therefore be hereby marked "*advertisement*" in accordance with 18 U.S.C. Section 1734 solely to indicate this fact.

We dedicate this paper to Dr. Hans Winkler on the occasion of his 65th anniversary.

‡ To whom correspondence should be addressed. Tel.: 43-1-4277-64171; Fax: 43-1-4277-9641; E-mail: michael.freissmuth@meduniwien.ac.at.

[1] The abbreviations used are: GABA, γ-aminobutyric acid; CFP, cyan fluorescent protein; COPII, coat protein complex II; DRAP, donor recovery after acceptor photobleaching; ER, endoplasmic reticulum; FRET, fluorescence (Förster) resonance energy transfer; (r)GAT1, (rat) GABA transporter 1; PDZ domain, a domain originally found in the proteins PSD-95/Dlg/ZO-1; YFP, yellow fluorescent protein; MDCK, Madin-Darby canine kidney; HEK, human embryonic kidney; wt, wild type; GFP, green fluorescent protein.

Pepperkok (European Molecular Biology Laboratory, Heidelberg, Germany) and H. T. Marten (Genentech Inc., San Francisco, CA). The construction of CFP- and YFP-tagged versions of rGAT1 has also been described previously (5). Mutations were introduced by PCR. Carboxyl-terminal deletions were created by inserting a stop codon with an ApaI restriction site at the proper position. In the case of point mutations, the codon of the targeted amino acid was replaced by the appropriate triplet to generate the intended amino acid substitution. The codon was again inserted with an ApaI restriction site. The integrity of all constructs was verified be sequencing the entire reading frame.

Cell Culture and Transfection—HEK293 cells were cultured in Dulbecco's modified Eagle's medium supplemented with 10% fetal bovine serum, L-glutamine, and antibiotics. MDCK cells were cultured in Dulbecco's modified Eagle's medium supplemented with 10% fetal bovine serum, L-glutamine, nonessential amino acids, and antibiotics. PC12 cells were cultured in Optimem-1 medium supplemented with 10% horse serum, 5% fetal bovine serum, L-glutamine, and antibiotics. Media were changed every other day. For experiments with HEK293 and MDCK cells, 0.3×10^6 cell (unless indicated otherwise) were plated into 6-well plates. For microscopy, cells were seeded on poly-D-lysine-coated glass coverslips at the same cell density. The $CaPO_4$ precipitation method was used to transiently transfect HEK293 and MDCK cells. The transfection efficiencies were 50–70 and 5–10% in HEK293 and MDCK cells, respectively. If not otherwise indicated, transfections were done 24 h after cell seeding. PC12 cells were seeded at a density of 0.15×10^6 cells on glass coverslips coated with collagen. If differentiation was to be induced, the medium was changed on the next day to Optimem-1 medium supplemented with 5% horse serum, L-glutamine, antibiotics, and 50 ng/ml nerve growth factor to induce differentiation. After 48 h, PC12 cells were transfected using LipofectAMINE Plus™ (Invitrogen). The transfection efficiency was 5–10%. Fluorescence microscopy was carried out 48 h later. Hippocampal neurons were prepared from neonatal rats as in Ref. 8. Glial cells were depleted by a 16-h incubation in the presence of 1 μM cytarabine (AraC). Neurons were transfected with LipofectAMINE 2000™ (Invitrogen) in 6-well dishes containing 3×10^5 dissociated cells. The expression of YFP-tagged GAT1 and the appropriately mutated forms was visualized by fluorescence microscopy 24–48 h after transfection.

Fluorescence Resonance Energy Transfer (FRET) Microscopy—Three methods were used to detect FRET: (i) donor photobleaching, (ii) donor recovery after acceptor photobleaching (DRAP), and (iii) the three-filter method to calculate net FRET. The setup has been described in detail elsewhere (6).

Donor photobleaching FRET was done by continuous illumination for 60 s using a mercury arc lamp (Zeiss HBO 100-watt intensity) with the CFP filter settings (excitation = 440 nm, dichroic mirror = 455 nm, emission = 480 nm). An image was captured every 3 s. This procedure bleached the donor (CFP) to less than 20%. Regions of interest were selected, and the time-dependent decrease in fluorescence emission intensity was quantified. The resulting decay curves were fitted to the equation of a single exponential decay approaching a constant value ($=A_0 \cdot e^{-kt}$). A_0 is the initial intensity, and k is the decay constant. The photobleaching lifetime (τ) was calculated from $\tau = 1/k$.

To measure DRAP we acquired a CFP image before (I_b) and after (I_a) photobleaching using the YFP setting for 90 s (excitation = 500 nm, dichroic mirror = 525 nm, emission = 535 nm). DRAP was quantified by FRET efficiency (E) as described by Miyawaki *et al.* (9) according to the equation $E = (I_a - I_b)/I_a$.

The three-filter method was done according to Youvan *et al.* (10). In brief, images were taken using the FRET filter (I_{FRET}; excitation = 440 nm, dichroic mirror = 455 nm, emission = 535 nm), CFP filter (I_{CFP}), and YFP filter settings (I_{YFP}). Background fluorescence was subtracted from all images; net FRET (nF) was calculated using the equation: $nF = I_{FRET} - (\alpha \times I_{YFP}) - (\beta \times I_{CFP})$ where α and β represent the bleed-through values for YFP (4%) and for CFP (34%).

Surface Biotinylation—HEK293 cells were transfected with YFP-tagged versions of GAT1-wt and GAT1-Δ27. 24 h later, transfection efficiencies were monitored with the fluorescence microscope. Subsequently cells were incubated with 2 mg/ml membrane impermeable sulfo-*N*-hydroxysuccinimide biotin for 20 min. Incubation was done at 4 °C to prevent endocytosis. The reaction was terminated by the addition of 50 mM glycine for 40 min at 4 °C. Cells were collected and lysed in buffer (100 mM Tris-Cl, pH 7.4, 150 mM NaCl, 1 mM EDTA, 1% Triton X-100, 1% sodium deoxycholate, 0.1% SDS, 1 μg/ml leupeptin, 1 μg/ml aprotinin, 250 μM phenylmethylsulfonyl fluoride). The lysate was centrifuged at $20{,}000 \times g$ (4 °C for 30 min) to remove insoluble material. The lysates were incubated overnight with an anti-GFP serum (full-length A.v. polyclonal antibody, Clontech) at 4 °C. Protein A-Sepharose was added for an additional 3 h. Protein was eluted from beads by treatment with SDS sample buffer for 30 min at 45 °C. Proteins were resolved on a 7% SDS-polyacrylamide gel and transferred onto a nitrocellulose membrane. YFP-GAT1 versions were detected with a monoclonal anti-GFP antibody (Clontech). After stripping, biotinylation was detected with horseradish peroxidase-streptavidin (2 μg/μl).

GABA Uptake—3×10^5 HEK293 cells were plated into 6-well plates. On the next day, cells were transfected; 24 h later, they were transferred to 48-well plates. GABA uptake was determined as outlined in detail elsewhere (6) in a final volume containing the concentrations of [ǂH]GABA (specific activity ranging from 72 to 0.07 Ci/mmol) indicated in the figures and legends. The incubation lasted for 3 min. The blank was determined in the presence of 100 μM tiagabine. Uptake was quenched by adding 1 ml of ice-cold Krebs-HEPES buffer. Cells were lysed in 1% SDS.

RESULTS

Membrane Targeting of GAT1 Is Disrupted by Deletion of 37 Amino Acids of the Carboxyl Terminus—To monitor the cellular localization of our various GAT1 constructs, we generated fusion proteins in which the GFP variants (YFP or CFP) were fused to the amino terminus of GAT1. Our previous experiments showed that the addition of a fluorescent protein to the transporter did not interfere with membrane targeting or affect the functional properties (that is the affinity for substrates and inhibitors as well as the velocity of substrate translocation) or the endocytosis and recycling of GAT1 in response to protein kinase C activation (6). Under the transfection conditions used, wild type YFP-rGAT was almost exclusively visualized at the cell surface in transiently transfected HEK293 cells (Fig. 1*A*). In contrast, if the carboxyl-terminal 37 amino acids were removed, the resulting truncated transporter CFP-rGAT-Δ37 was not found at the plasma membrane but was completely retained within the cell (Fig. 1*B*). We stained transiently transfected cells with the selective dye ER Tracker Blue-White DPX (Fig. 1*F*, *green* pseudocolor) and also recorded the fluorescence emitted by YFP-rGAT-Δ37 (Fig. 1*E*, *red* pseudocolor). The overlay of both images resulted in uniform yellow coloring of those cells that expressed the transporter (Fig. 1*G*). This colocalization confirmed that the intracellular compartment in which rGAT-Δ37 resided was the endoplasmic reticulum.

The Carboxyl-terminally Truncated Mutant Interacts with Wild Type GAT1—We have reported previously that GAT1 assembles into constitutive oligomers, which are formed in the endoplasmic reticulum (5, 6). This has also been proposed for other neurotransmitter transporters (11). Oligomer formation can thus be viewed as an endoplasmic reticulum (ER) quality control mechanism. This is underscored by the observation that membrane targeting of GAT1 is absent when oligomerization is disrupted (6). We therefore investigated whether the observed intracellular retention of CFP-GAT1-Δ37 is due to defective oligomerization. We co-transfected HEK293 cells with CFP-GAT1-Δ37 (donor) and YFP-rGAT-wt (acceptor). To measure FRET we used donor photobleaching to calculate the decay time of fluorescence intensity as well as DRAP to calculate the FRET efficiency. In the first approach, energy transfer protects the donor against bleaching because energy is absorbed by the acceptor. Conversely DRAP relies on the fact that photodestruction of the acceptor results in enhanced fluorescence of the donor due to interruption of energy transfer. Both methods allow for quantification and thus for a statistical comparison. Fig. 2*A* shows a representative set of bleaching curves from one experimental day; the concomitant expression of YFP-tagged wild type GAT1 (Fig. 2*A*, *open symbols*) caused a delay in photobleaching when compared with cells that only expressed the CFP-tagged truncated GAT1-Δ37 (Fig. 2*A*, *open symbols*). As can be seen from Fig. 2*B*, there was a statistically significant difference in the average photobleaching lifetimes (τ) determined in the absence and presence of acceptor (that is wild

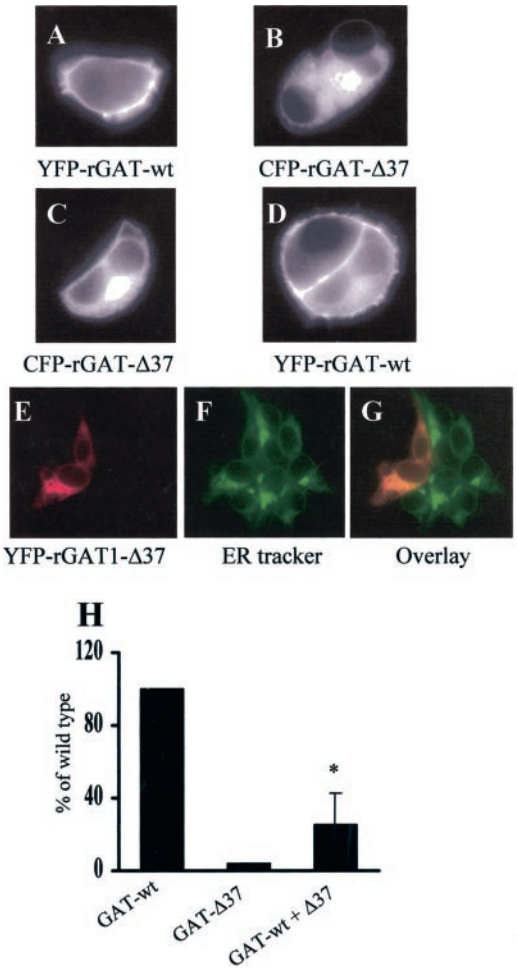

FIG. 1. **Subcellular localization of wild type and mutant GAT1 in HEK293 cells.** HEK293 cells were transiently transfected with plasmids encoding YFP-tagged wild type GAT1 (*A*) or CFP-tagged GAT1 lacking the last 37 amino acids (*B*). Images were captured 24 h later with the appropriate filter settings. *C* and *D*, HEK293 cells co-transfected with plasmids encoding YFP-tagged wild type GAT1 and CFP-tagged GAT1-Δ37. The CFP (*C*) or YFP (*D*) filter settings were used to visualize the respective protein. *E*, *F*, and *G*, HEK293 cells were transiently transfected with a plasmid encoding YFP-tagged rGAT1-Δ37. After 24h, the cells were incubated with 600 nM ER Tracker Blue-White DPX for 30 min, and the fluorophores were visualized using filter settings for YFP for the GAT1 mutant (*E*, *red* color) and CFP for the ER Tracker Blue-White DPX (*F*, *green* color). Both images were overlaid using the MetaMorph software (*G*). *H*, HEK293 cells were transfected either with YFP-tagged wild type GAT1 (*left bar*), CFP-tagged GAT1-Δ37 (*middle bar*), or with both (*right bar*). Uptake of [^{3}H]GABA (10 μM) was determined as outlined under "Experimental Procedures." To normalize for interassay differences in transient transfections, [^{3}H]GABA uptake by cells that expressed solely the wild type transporter was used as a reference and set as 100%. This value amounted to 325 ± 95 pmol·min^{-1}·10^{-6} cells. Results are means ± S.E. from four independent experiments that were carried out in parallel and done with triplicate determinations. The *asterisk* indicates a significant difference from the wild type at $p = 0.001$ (unpaired t test).

type GAT1). Similarly we also detected a robust FRET by DRAP (Fig. 2*C*). In the absence of FRET (*i.e.* in the absence of an acceptor), there was also a modest decrease in fluorescence intensity of the donor; this is due to the fact that bleaching with the YFP settings results in slight but appreciable cross-bleaching of CFP.

Detection of FRET using the three-filter method offers the advantage that it visualizes the cellular compartment in which the proposed protein-protein interaction takes place. Fig. 3 shows that CFP-GAT1-Δ37 and YFP-rGAT-wt indeed interact intracellularly. The results of our FRET experiments clearly rule out the possibility that retention is due to defective oligomerization. Instead the observations indicate that the carboxyl-terminal deletion mutant is able to directly interact with the wild type transporter. Thus, due to its defective surface expression, the truncated GAT1-Δ37 apparently also traps the wild type protein within the cell. This interpretation was verified by exploiting the fact that YFP and CFP can be visualized separately within the same cell by the appropriate filter sets. Cells were co-transfected with plasmids encoding wild type YFP-GAT1 and CFP-GAT1-Δ37. This resulted in intracellular retention of the wild type transporter (Fig. 1*D*) in cells that also expressed the truncated transporter (Fig. 1*C*). In contrast, in those cells that did not express the deletion mutant, wild type YFP-GAT1 was found at the membrane (Fig. 1*D*, exemplified by the *upper cell*). Transporters that are retained within the cell are irrelevant to the uptake of [^{3}H]GABA. Thus, coexpression of the carboxyl-terminally truncated mutant ought to abrogate transport mediated by the wild type transporter. This was the case. HEK293 cells expressing only YFP-rGAT-wt displayed a robust uptake of [^{3}H]GABA (Fig. 1H, *left-hand bar*), while cells coexpressing CFP-rGAT-Δ37 did not show any significant uptake of radioactive substrate (Fig. 1*H*, *right-hand bar*). As predicted from the absence of surface-associated fluorescence (Fig. 1*B*), cells that only expressed CFP-rGAT-Δ37 did not accumulate [^{3}H]GABA (Fig. 1*E*, *middle bar*). To rule out that defective membrane targeting was due to misfolding of the protein, we performed GABA uptake experiments in membrane vesicles prepared from appropriately transfected cells (6). Under these conditions, CFP-GAT1-Δ37 and wild type CFP-GAT1 translocated the substrate [^{3}H]GABA with similar affinity (K_m = 7.6 ± 4.8) and comparable velocity (data not shown).

CFP-GAT1-Δ36 Is Not Inserted into the Plasma Membrane—It has been reported previously that deletion of 36 amino acids from the carboxyl terminus of GAT1 did not interfere with membrane targeting of the transporter (7). GAT1-Δ37 and GAT1-Δ36 differ by a leucine residue at position 563. We aligned the carboxyl termini of several Na^+/Cl^--dependent neurotransmitter transporters (Fig. 4*A*) and noted that Leu^{563} was conserved among many family members and was replaced by phenylalanine in serotonin transporter and isoleucine in dopamine transporter, which are nevertheless hydrophobic amino acids. Because of the conserved nature of this amino acid, we surmised that Leu^{563} played an essential role in the targeting process. We therefore generated CFP-GAT1-Δ36 and expressed this mutant in HEK293 cells. The representative example shown in Fig. 4*B* illustrates that the protein was only found in intracellular compartments. Expression of CFP-GAT1-Δ36 also failed to confer [^{3}H]GABA uptake to cells (not shown). Because Perego *et al.* (7) had expressed their construct in the polarized epithelial cell line MDCK, we also used this cell line. In MDCK cells wild type GAT1 was efficiently targeted to the cell surface (Fig. 4*C*). In contrast, CFP-GAT1-Δ36 only accumulated within the cell (Fig 4*D*). MDCK cells and other polarized epithelial cells are used as a surrogate for neuronal cells. Because neurotransmitter transporters are expressed predominantly in neurons, we also investigated the fate of CFP-GAT1-Δ36 in differentiated PC12 cells. In these cells, YFP-GAT1-wt was present exclusively in the plasma membrane and was highly enriched at the sites of sprouting neurites extensions (Fig. 4*E*). This is to be expected because GAT1 is enriched in the axonal compartment (12). On the other hand, as in the other cell lines, CFP-GAT1-Δ36 was only found within the differentiated PC12 cell (Fig. 4*F*). Finally we performed the same experiments in hippocampal neurons because these are among the neurons that express GAT1 endogenously (13). In these cells, the wild type GAT1 was found on the somatic cell

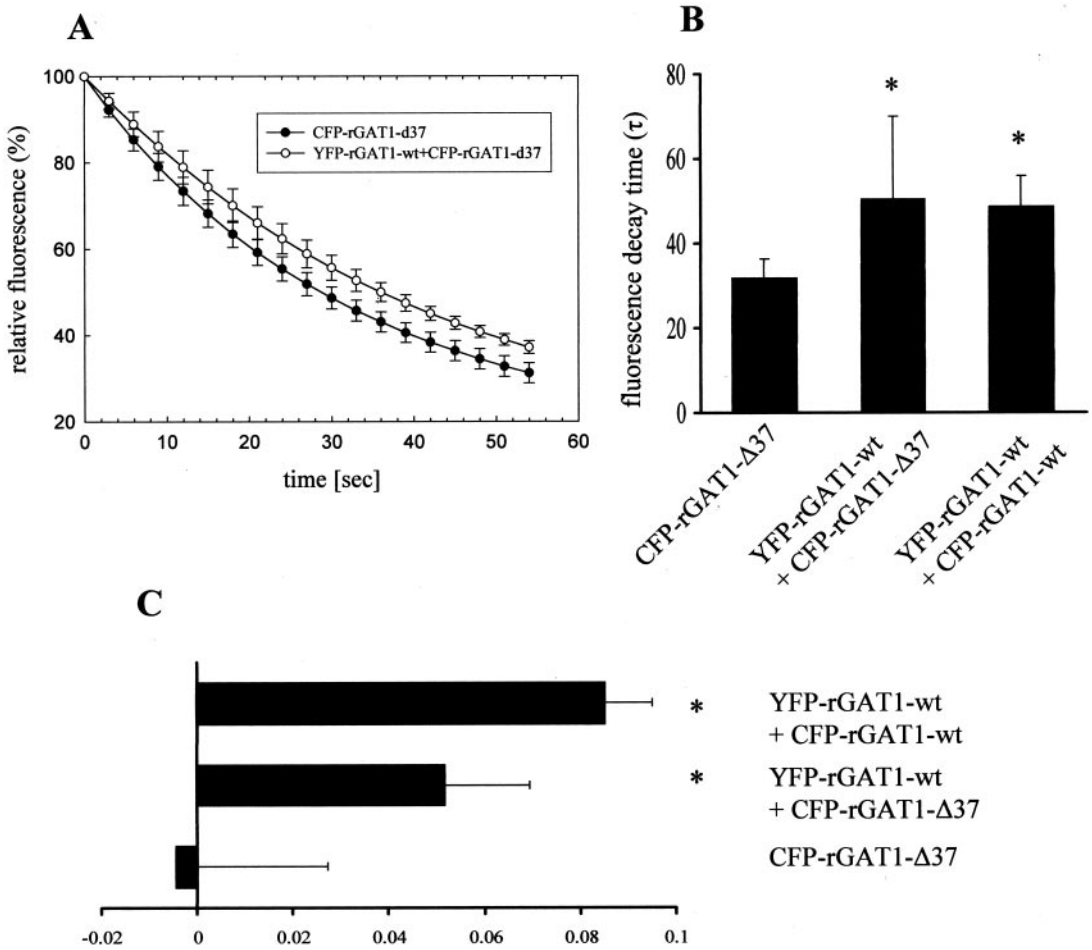

FIG. 2. **FRET microscopy of YFP-tagged wild type GAT1 and CFP-tagged GAT1-Δ37.** *A* and *B*, donor photobleaching FRET. HEK293 cells were transfected with a plasmid encoding CFP-tagged GAT1-Δ37 (*closed symbol*) alone or in combination with that coding for YFP-tagged wild type (*open symbol*). After 24–48 h, photobleaching of the donor (CFP) was achieved by illuminating the center of the visual field with a mercury arc lamp (Zeiss HBO, 100 watts) for 60 s. An image was captured and digitized every 3 s; the decay of fluorescence intensity was followed in consecutive images over regions of interest using the MetaFluor software package. The initial fluorescence at time = 0 s was set as 100%. The data points represent the average ± S.D. from decay curves that were recorded on the same experimental day in eight cells each. The photobleaching lifetime (τ) was calculated by fitting the decline in intensity to an equation describing a monoexponential decay. *B* shows the averages from a total of 24 cells each (recorded on three different experimental days). *C*, DRAP-FRET. Evaluation of FRET efficiency. HEK293 cells were transfected with the plasmid coding for CFP-tagged GAT1-Δ37 alone or in combination with a plasmid encoding YFP-tagged wild type transporter as indicated. Bleaching was achieved by illuminating the center of the visual field with a mercury lamp for 90 s. Images with the CFP filter settings were captured before and after photodestruction of the acceptor. FRET efficiency was calculated as indicated under "Experimental Procedures." Results presented are means ± S.E. (n = 24 in *B* and 12 in *C*). The *asterisk* indicates a significant difference at $p \leq 0.001$ (unpaired t test).

surface (Fig. 4*G*, *left*) and in neurite extensions (Fig. 4*G*, *right*). Somatic expression is most likely due to overexpression of the transporter. More importantly, CFP-GAT1-Δ36 was not visualized at the cell surface of hippocampal neurons (Fig. 4*H*). Based on these observations, we conclude that, despite its high degree of conservation, Leu^{563} is not essential for targeting the transporter to the plasma membrane.

Plasma Membrane Targeting Relies on Two Different Regions in GAT1 Carboxyl Terminus—It is evident that the amino acids that are important for targeting must lie in more distal portions of the carboxyl terminus. Thus, we elongated GAT1-Δ37 stepwise by 10 amino acids. CFP-GAT1-Δ27 was inserted into the cell membrane as was CFP-rGAT-Δ17 and -Δ7 (Fig. 5*A*, *B*, and *C*, respectively). Interestingly much of the protein was nevertheless located intracellularly. We verified that all these proteins were functional by performing saturation experiments on transiently transfected HEK293 cells. Fig. 5*F* shows a set of representative saturation curves that were obtained in parallel. The calculated K_m values for the mutants did not differ significantly from that of the wild type (wild type = 8.7 ± 2.6, GAT1-Δ27 = 9.3 ± 3.1, GAT1-Δ17 = 6.7 ± 2.3, GAT1-Δ7 = 9.9 ± 3.7).

To further prove that membrane expression of CFP-rGAT-Δ27 is indeed lower than that of the wild type protein, we transfected HEK293 cells with increasing amounts of plasmid DNA. Uptake of [^{3}H]GABA was determined at a GABA concentration (10 μM) that was within the K_m concentration range. This resulted in a robust signal-to-noise ratio without requiring the use of excessive amounts of radioactive tracer. Because the K_m values of the various mutated versions of GAT1 were virtually identical (see Fig. 5*F*), the transport velocity determined at this concentration only reflects the level of transporter at the cell surface. As can be seen from Fig. 5*G*, there was a hyperbolic relation between the amount of plasmid DNA and transport velocity for both wild type YFP-GAT1 (*open diamonds*) and CFP-rGAT1-Δ27 (*closed triangles*), and the amount of DNA required to support half-maximum expression of the two transporters did not differ appreciably. However, transport velocity was significantly lower in cells expressing CFP-rGAT1-Δ27 than in those expressing YFP-rGAT-wt, and this was not overcome by the addition of excess plasmid (Fig. 5*G*). This indicated that plasma membrane expression of the mutant was lower than that of the wild type transporter. On average the surface expression of CFP-rGAT1-Δ27 was 50% of that of the corre-

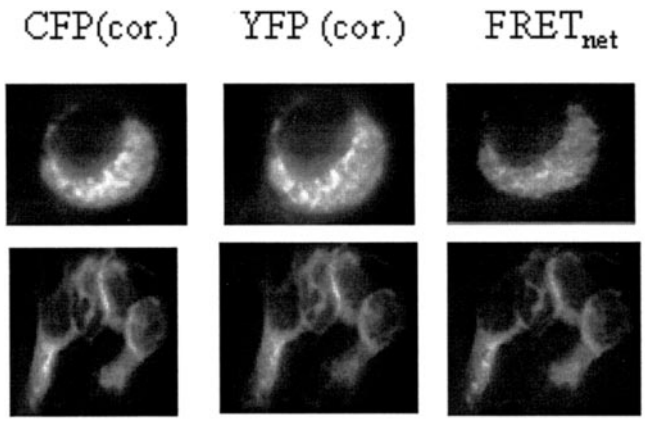

FIG. 3. **Three-filter FRET microscopy of HEK293 cells expressing YFP-tagged wild type GAT1 and CFP-tagged GAT1-Δ37.** Cells were transfected with a combination of YFP-tagged wild type GAT1 and CFP-tagged GAT1-Δ37. Images were acquired using the CFP, YFP, and FRET filter setting as outlined under "Experimental Procedures." Background fluorescence was subtracted from all images. CFP and YFP images were corrected for the bleed-through factors (36% for the donor and 4% for the acceptor). The corrected CFP and YFP intensities were subtracted from the FRET image resulting in the net FRET image shown at the *right* side of the figure. The *upper* and *lower row* show a representative selection of a cell or cells, respectively, to illustrate that FRET is exclusively seen in intracellular compartments but not at the cell surface. *cor.*, corrected.

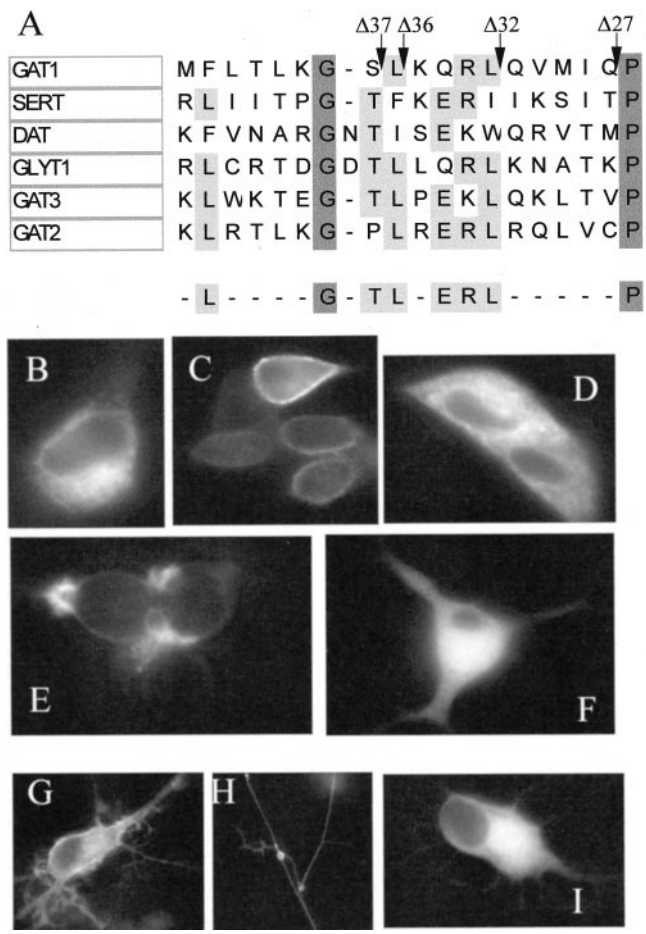

FIG. 4. **Localization of YFP-tagged wild type GAT1 and CFP-tagged GAT1-Δ36 in HEK293 cells, MDCK cells, differentiated PC12 cells, and hippocampal neurons.** *A*, alignment of the proximal part of the carboxyl terminus of GAT1 with the respective regions in the serotonin transporter (*SERT*), the dopamine transporter (*DAT*), the glycine transporter type 1 (*GLYT1*), and the GABA transporter types 2 and 3 (*GAT2* and *GAT3*) to illustrate the conserved leucine residue. *Arrows* show the site of truncation for the indicated mutants. *B*, HEK293 cells were transfected with CFP-tagged GAT1-Δ36. *C* and *D*, MDCK cells were transfected with YFP-tagged wild type GAT1 (*C*) or CFP-tagged GAT1-Δ36 (*D*). *E* and *F*, PC12 cells were subjected to differentiating conditions for 48 h prior to transfection with YFP-tagged wild type GAT1 (*E*) or CFP-tagged GAT1-Δ36 (*F*). Images were captured 24 (*B–D*) and 48 h (*E* and *F*) after transfection. *G* and *H*, hippocampal neurons were transfected with YFP-tagged wild type GAT1 (*G*) or CFP-tagged GAT1-Δ36 (*H*). Images were acquired 24 h later.

sponding wild type transporter. To confirm the results of this experiment we measured the amount of GAT1 at the cell surface by biotinylation with the membrane-impermeable reagent sulfo-*N*-hydroxysuccinimide biotin. HEK293 cells were transiently transfected with a plasmid driving either the expression of YFP-GAT1-wt (7.5 μg/10-cm dish) or the YFP-GAT1-Δ27 (15 μg/10-cm dish). The levels of immunoprecipitated YFP-tagged transporter were estimated by immunoblotting; the amount of YFP-GAT1-Δ27 was ~2-fold higher than that of YFP-GAT1-wt (Fig. 5*H*, *upper panel*). However, the levels of biotinylated transporter were comparable (Fig. 5*H*, *lower panel*). Taken together, these observations are consistent with the findings in the uptake experiments and indicate that the uptake velocity of GAT1-Δ27 (and by inference of the other truncated mutants) is reduced because of the decreased cell surface expression rather than because the carboxyl terminus affects the transport rates.

Based on these findings we concluded that the 10 additional amino acids by which GAT1-Δ27 differed from GAT1-Δ37 must contain a signal that supports trafficking of the transporter to the plasma membrane albeit to a limited extent. Upon further inspection of the amino acid sequence between Leu^{563} and Gln^{572} we found a moderately conserved QRL motif. Adding back these amino acids results in CFP-rGAT-Δ32. This construct, however, was not targeted to the plasma membrane in HEK293 cell (Fig. 5*D*) and did not support cellular uptake of [^{3}H]GABA (data not shown). Thus the residues QVMIQ represent the crucial portion, while the adjacent preceding residues are irrelevant to the process of ER export. In this context, it is worth mentioning that extending the carboxyl terminus up to position Δ7 (or rather Δ3, see below) did not enhance surface expression as assessed by cellular [^{3}H]GABA uptake (Fig. 5*G*).

A substantial amount of rGAT-Δ27 was located intracellularly. Fluorescence emitted by CFP-rGAT-Δ27 (Fig. 6*A*) and the ER Tracker dye (Fig. 6*B*) colocalized when overlaid (Fig. 6*C*). Thus, the intracellular compartment in which rGAT-Δ27 accumulated was the endoplasmic reticulum.

Dihydrophobic motifs are well known ER export motifs (14). We surmised that such a motif was located within the sequence essential for export of rGAT1 (QVMIQ). To address this conjecture we created additional deletion mutants. HEK293 cells were transiently transfected with CFP-rGAT-Δ31, CFP-rGAT-Δ30, CFP-rGAT-Δ29, and CFP-rGAT-Δ28. Surface expression was assessed by measuring [^{3}H]GABA uptake into intact cells. Only cells expressing CFP-rGAT-Δ28 displayed a robust GABA uptake (Fig. 6*D*) that was similar in magnitude to that obtained with rGAT-Δ27 (*cf.* Fig. 5*G*). Accordingly CFP-rGAT-Δ28 was also detected at the cell surface expression by fluorescence microscopy, while the other mutants were not (data not shown).

It has recently been suggested that the last three amino acids of GAT (AYI) comprise a PDZ interaction domain important for interaction with the membrane-associated guanylate kinase family member Pals-1 (15). This implies that this AYI motif plays a role in the targeting process. HEK293 cells do not express Pals-1 (16). Nevertheless it is conceivable that a related protein recognizes this motif and thereby supports membrane targeting and/or insertion. Thus we constructed a CFP-tagged version of GAT1 lacking the last three amino acids. The K_m value for this mutant did not differ from that of the wild type transporter (wild type = 8.7 ± 2.6, GAT1-Δ3 = 10.5 ± 3.8).

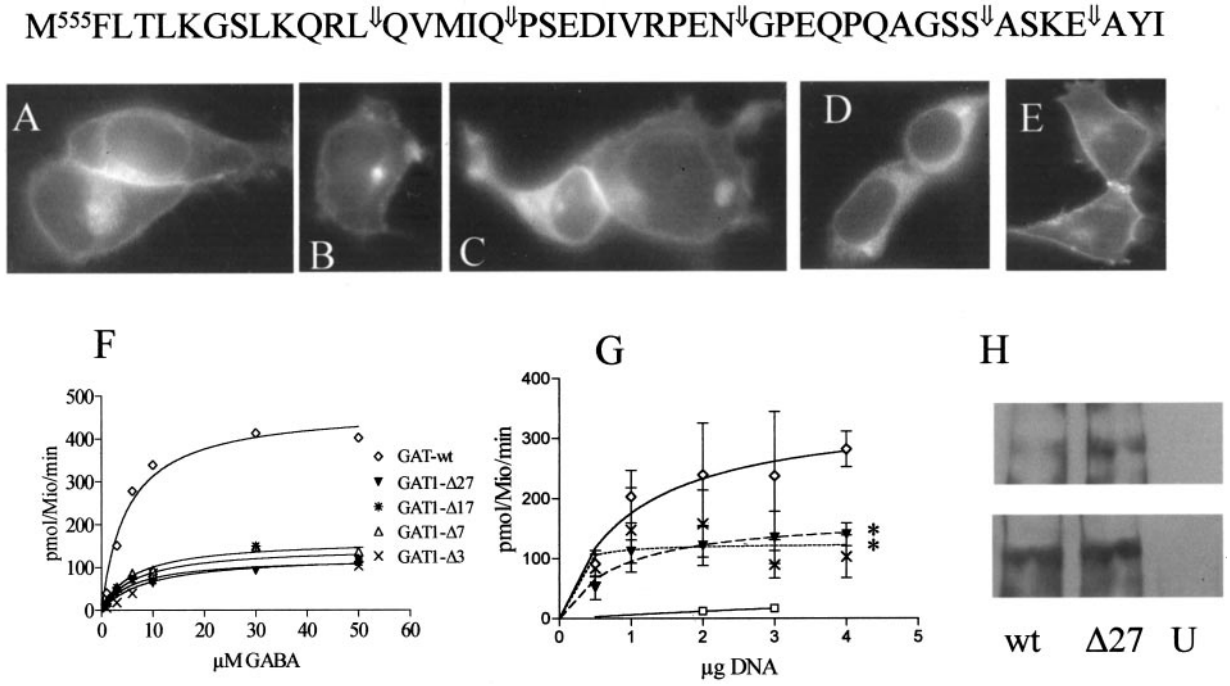

FIG. 5. **Subcellular localization, transport velocity, and surface biotinylation as an estimate for surface expression of CFP-tagged carboxyl-terminally truncated GAT1 mutants.** HEK293 cells were transiently transfected with plasmids encoding CFP-tagged GAT1-Δ27 (*A*), GAT1-Δ17 (*B*), GAT1-Δ7 (*C*), GAT1-Δ32 (*D*), and GAT1-Δ3 (*E*). The sequence of the carboxyl terminus of GAT1 (starting with Met^{555}) is shown on *top* of the micrographs; the *arrows* mark the sites of truncation. *F*, saturation curves for YFP-tagged wild type GAT1 as well as for CFP-tagged GAT1-Δ27, GAT1-Δ17, GAT1-Δ7, and GAT1-Δ3; assay conditions were as outlined under "Experimental Procedures." Data are from a representative experiment that was carried out in parallel and done in triplicate. Two additional experiments gave comparable results. *G*, HEK293 cells were transfected with increasing amounts of plasmids encoding YFP-tagged wild type GAT1 (*diamonds*), CFP-tagged GAT1-Δ27 (*triangles*), GAT-Δ3 (*crosses*), and GAT-Δ37 (*squares*). The total DNA amount was kept constant. Uptake of [^{3}H]GABA (10 µM) was assayed as in *F*. Results are means ± S.E. ($n = 3$). *Asterisks* indicate statistically significant differences of truncated GAT1 from the wild type control at $p < 0.05$ (one-way analysis of variance followed by Tukey's test). *H*, HEK293 cells were transiently transfected with plasmids encoding YFP-GAT1-wt (*wt*; 7.5 µg/10-cm dish) or YFP-GAT1-Δ27 (*Δ27*; 15 µg/10-cm dish). *U* indicates a lysate from HEK293 cells that were not transfected. Surface biotinylation, immunoprecipitation, and immunoblotting were performed as outlined under "Experimental Procedures."

The cellular distribution and the extent of membrane expression of CFP-rGAT-Δ3 was very similar to that observed with CFP-rGAT-Δ27 as determined by fluorescence microscopy (Fig. 5*E*) and by [^{3}H]GABA uptake with increasing amounts of plasmid transfected (Fig. 5*G*). Based on these observations, we conclude that the carboxyl terminus of GAT1 carries two separate targeting signals. The first is the hydrophobic motif located between Val^{569} and Ile^{571}, and the second is represented by the last three amino acids.

It is conceivable that each signal acts independently. Alternatively there may be a hierarchy among both signals. To differentiate between these two possibilities, we fused the AYI motif to CFP-GAT1-Δ37 and transfected it into HEK293 cells. If both signals acted independently from each other, addition of this motif should drive membrane expression of the truncated protein. The result was unequivocal: addition of AYI did not rescue GAT1-Δ37 from intracellular retention (Fig. 7*A*). Reports in the literature point to an important role of amino acids that are located upstream of the PDZ interaction motif (17). To rule out the effect of any other amino acids upstream of the AYI motif, we fused the last 10 amino acids to CFP-GAT1-Δ37 (Fig. 7*B*) and to CFP-GAT1-Δ32 (Fig. 7*C*). Both constructs did not reach the plasma membrane. If there is a hierarchy of both signals, the mutation of the proximal signal ought to cause retention even if the distal signal is present in its correct context, that is the otherwise intact carboxyl terminus. Therefore we replaced the three hydrophobic amino acids (^{569}VMI^{571}) by serines (YFP-rGAT1-SSS). This mutant did not reach the plasma membrane (Fig. 7*D*). Thus the two signals act in a hierarchical manner.

The Terminal Three Amino Acids of GAT1 Represent a PDZ Interaction Domain—It was inferred by McHugh *et al.* (15) that the terminal three amino acids (AYI) comprise a PDZ interaction domain. The formal proof for this conjecture was not provided. The consensus sequence for a PDZ interaction domain is (T/S)*X*ϕ (ϕ indicates a hydrophobic amino acid) for interaction with class I PDZ domains and $\phi X\phi$ for interaction with class II PDZ domains. The sequence AYI implies an interaction with a class II PDZ domain. The presence of a terminal hydrophobic residue is crucial to support interaction with the PDZ domain. We therefore mutated the terminal isoleucine to alanine. Despite its small size (by comparison with isoleucine), alanine is not expected to disrupt the interaction with the PDZ domain because it is non-polar. In contrast substitution with a polar amino acid ought to abrogate the interaction with a PDZ domain. Hence we replaced the isoleucine by a glutamate. Cell surface expression of these two point mutants was assessed by fluorescence microscopy (Fig. 8, *A* and *B*) and by measuring cellular uptake of [^{3}H]GABA (Fig. 8*C*). CFP-GAT1-AYA (*i.e.* the mutant in which isoleucine was substituted by alanine) was predominantly if not exclusively visualized at the cell surface (Fig. 8*A*). In contrast, copious amounts of CFP-GAT1-AYE were detected in intracellular compartments (Fig. 8*B*) resulting in pictures that were comparable to those found with CFP-rGAT1-Δ3 (*cf.* Fig. 5*E*). These results were confirmed by cellular [^{3}H]GABA uptake assays, which reflect average surface expression in the entire cell population of the dish and thus eliminate observer bias (Fig. 8*C*): [^{3}H]GABA uptake in cells expressing CFP-GAT1-AYA was comparable to those expressing wild type GAT1. In contrast, transport velocity was reduced

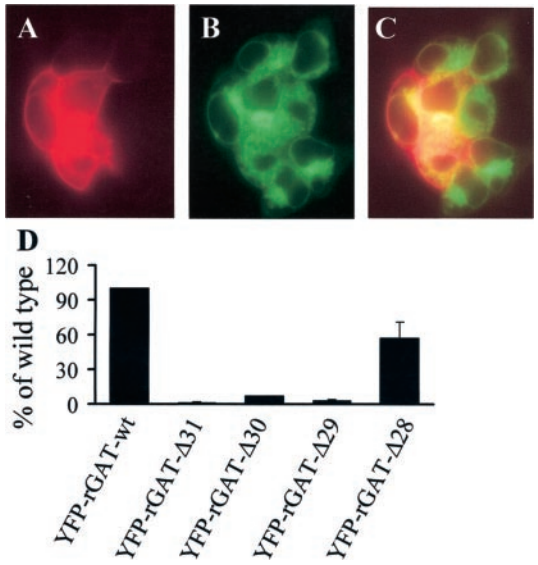

FIG. 6. **Subcellular localization of GAT1-Δ27 and characterization of the proximal motif in rGAT1 carboxyl terminus.** *A*, *B*, and *C*, HEK293 were transiently transfected with YFP-tagged rGAT-Δ27. On the next day cells were incubated with ER Tracker Blue-White DPX (600 nM) for 30 min. The fluorophores were visualized using the YFP filter setting for the GAT1 mutant (*red* color in *A*) and CFP filter settings for the ER Tracker Blue-White DPX (*green* color in *B*). Both images were overlaid using the MetaMorph software (*C*). *D*, HEK293 cells were transiently transfected with plasmids encoding CFP-tagged rGAT1-Δ31, -Δ30, -Δ29, and -Δ28. Uptake of [^{3}H]GABA (10 μM) was determined as outlined under "Experimental Procedures." To normalize for interassay differences in transient transfections, [^{3}H]GABA uptake by cells that expressed solely the wild type transporter was used as a reference and set as 100%. This value amounted to 157 ± 60 pmol·min^{-1}·10^{-6} cells. Results are means ± S.E. from three independent experiments that were carried out in parallel and done with triplicate determinations. The *asterisk* indicates a significant difference from the wild type at $p = 0.001$ (unpaired t test).

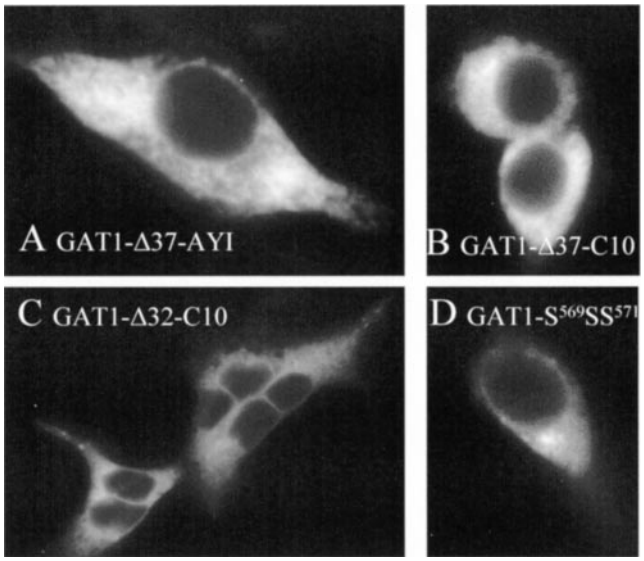

FIG. 7. **Hierarchy of signals in the carboxyl terminus of GAT1.** *A* and *B*, HEK293 cells were transfected with a plasmid driving the expression of CFP-tagged GAT1-Δ37 onto which the last three amino acids (*A*, *GAT1-Δ37-AYI*) or the last 10 amino acids (*B*, *GAT1-Δ37-C10*) were grafted. *C*, the last 10 amino acids were fused to CFP-rGAT1-Δ32 (*CFP-rGAT1-Δ32-C10*). *D*, YFP-tagged GAT1 in which the VMI motif was replaced by three serines (GAT1-^{569}SSS^{571}).

by about 50% in cells expressing CFP-rGAT1-AYE and CFP-rGAT1-Δ3. It is worth pointing out that the HEK293 cells were transfected in parallel with 2 μg each of the appropriate plasmid. This amount of plasmid sufficed to saturate cell surface

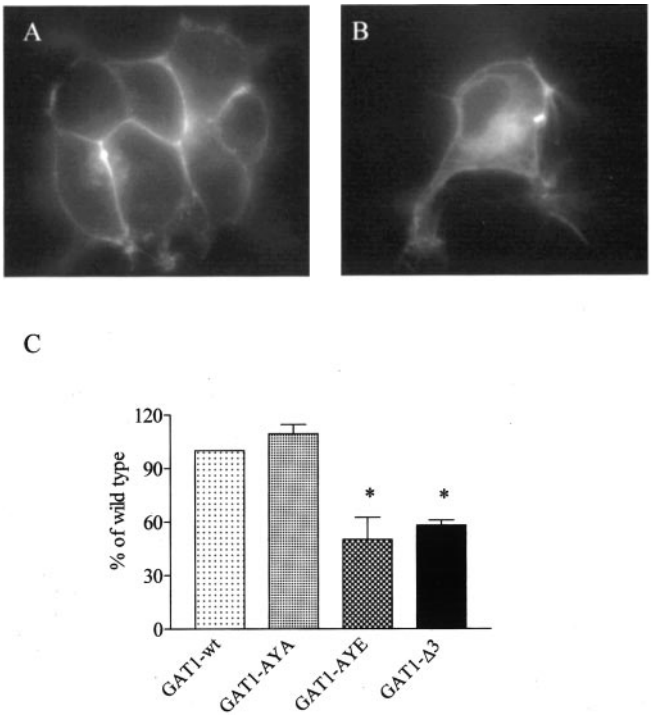

FIG. 8. **Subcellular localization and surface expression of wild type GAT1 and GAT1 constructs with mutations in their PDZ-binding motif.** HEK293 cells were transfected with CFP-tagged GAT1-AYA (*A*) and CFP-tagged GAT1-AYE (*B*). Images were acquired 24 h after transfection. *C*, transport velocity as an estimate of surface expression of GAT1 constructs. HEK293 cells were transiently transfected with plasmids encoding YFP-tagged wild type GAT1, CFP-tagged GAT1-AYA, GAT1-AYE, or GAT1-Δ3. Uptake of [^{3}H]GABA (10 μM) was determined as outlined under "Experimental Procedures." To normalize for interassay differences in transient transfections, [^{3}H]GABA uptake by cells that expressed solely the wild type transporter was used as a reference and set as 100%. This value amounted to 658 ± 147 pmol·min^{-1}·10^{-6} cells. Results are means ± S.E. ($n = 4$). Asterisks indicate statistically significant differences of truncated GAT1 from the wild type control at $p < 0.05$ (one-way analysis of variance followed by Tukey's test).

expression (Fig. 5*G*). Finally we also investigated the contribution of the hydroxyl group of tyrosine by replacing this residue with phenylalanine. This substitution did not have any appreciable effect (data not shown).

The PDZ Interaction Domain in GAT Carboxyl Terminus Is Not Necessary for Polarized Sorting—The fact that surface expression of CFP-rGAT1-Δ3 was lower than that of the wild type transporter implies that the PDZ domain is important for interaction with a rate-limiting factor, which might support membrane insertion. In this case, the protein must already be sorted en route to its definitive compartment. If this model were correct, the AYI motif should not play a role in the process of sorting because the interaction with the putative PDZ domain protein presumably only controls the rate of membrane insertion. Thus, the mutants that lack the PDZ interaction motif are expected to be targeted as efficiently to specialized cell surface destinations as the wild type protein. This prediction was verified in differentiating PC12 cells by comparing the sorting of the wild type transporter with that of constructs in which the PDZ interaction motif had been mutated or deleted. Indeed YFP-rGAT1-wt as well as CFP-rGAT1-Δ3, -AYA, and -AYE were all enriched at the sites of sprouting neurite extensions (Fig. 9, *A–D*). These results therefore confirm the conjecture that the proximal portion of the GAT1 carboxyl terminus suffices for sorting the protein to the correct compartment.

Sec24D Binds to the Carboxyl Terminus of GAT1—Export of proteins from the endoplasmic reticulum occurs by bulk flow or

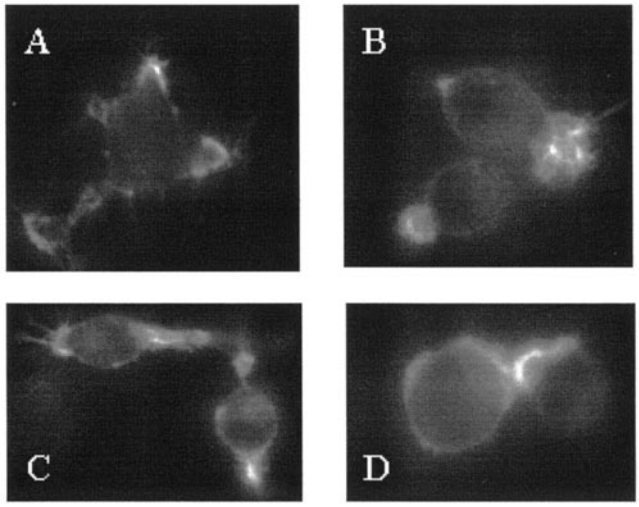

FIG. 9. **Subcellular localization of wild type GAT1 and GAT1-Δ3, GAT1-AYA, and GAT1-AYE in differentiated PC12 cells.** PC12 cells were subjected to differentiating conditions for 48 h prior to transfection with plasmids encoding YFP-tagged wild type GAT1 (*A*), CFP-tagged GAT1-Δ3 (*B*), GAT1-AYA (*C*), or GAT1-AYE (*D*). Images were acquired 48 h after transfection. Data are representative for three independent transfections.

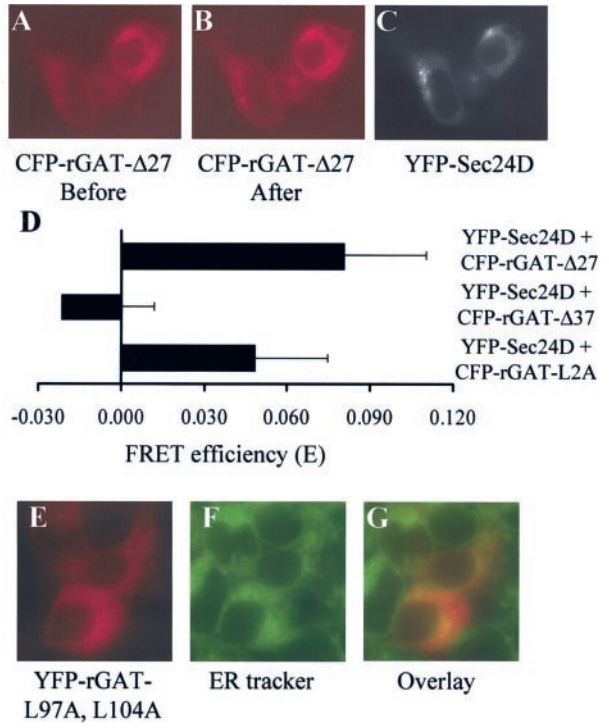

FIG. 10. **FRET microscopy of YFP-tagged Sec24p and CFP-tagged. DRAP-FRET experiments were performed as outlined under "Experimental Procedures."** *E*, *F*, and *G*, HEK293 were transiently transfected with YFP-tagged rGAT-L97A,L104A. On the next day cells were incubated with ER Tracker Blue-White DPX (600 nM) for 30 min. The fluorophores were visualized using the YFP filter setting for the GAT1 mutant (*red* color in *E*) and CFP filter settings for the ER Tracker Blue-White DPX (*green* color in *F*). Both images were overlaid using the MetaMorph software (*G*) GAT1 mutants. *A*, *B*, and *C*, representative set of images showing fluorescence intensity of CFP-rGAT1-Δ27 before (*A*) and after (*B*) photobleaching of the acceptor as well as an image of Sec24p-YFP (*C*). *D*, evaluation of FRET efficiency (abbreviated "*E*") in HEK293 cells transfected with plasmids encoding Sec24p-YFP in combination with CFP-rGAT1-Δ27 (*upper bar*), CFP-rGAT1-Δ37 (*middle bar*), or CFP-rGAT1-L97A,L104A (*lower bar*).

by recruitment of proteins of the ER export machinery to specific signals of the cargo protein (for a review, see Ref. 18). In the latter case proteins are sorted into coat protein complex II (COPII) vesicles. As rGAT1-Δ37 is retained in the endoplasmic reticulum although it is competent of forming oligomers, it is conceivable that it cannot bind to proteins of the COPII complex; rGAT1-Δ27, however, is exported because it can recruit the COPII constituents. In the COPII coat, Sec24 is thought to bind cargo molecules via a set of at least three distinct binding sites (19, 20). We therefore transfected HEK293 cells with plasmids encoding YFP-tagged Sec24D together with CFP-tagged versions of rGAT1-Δ37 and rGAT1-Δ27. DRAP was used to visualize any interaction. A representative set of fluorescence images is shown in Fig. 10, namely images captured for CFP-rGAT1-Δ27 prior to (Fig. 10*A*) and after bleaching of the acceptor YFP-Sec24D (Fig. 10*B*). The increase in fluorescence intensity was readily seen upon bleaching of the acceptor (*cf.* Fig. 10, *A* and *B*), and it was confined to those intracellular areas where YFP-Sec24D had accumulated (Fig. 10*C*). To allow for quantification, we calculated the FRET efficiency in each individual bleaching experiment. These data are summarized in Fig. 10*D*. It is evident that we failed to record any appreciable resonance energy transfer between CFP-rGAT1-Δ37 and YFP-Sec24D. Thus the observations were consistent with the interpretation that CFP-rGAT1-Δ27, but not CFP-rGAT1-Δ37, bound to YFP-Sec24D.

As an additional control we used the L97A,L104A mutant of rGAT1 that fails to form a homo-oligomer (6). A CFP-tagged version of this mutant was also retained in the endoplasmic reticulum as shown by colocalization with the ER Tracker dye (Fig. 10, *E–G*). The carboxyl terminus is identical in wild type GAT1 and in the L97A,L104A mutant. Therefore, the L97A,L104A mutant is expected to bind Sec24D because it accumulates in the endoplasmic reticulum. Thus, we coexpressed a CFP-tagged version of rGAT1-L97A,L104A with Sec24p-YFP in HEK293 cells and monitored the interaction by DRAP-FRET. The efficiency of resonance energy transfer between the two proteins was comparable to that seen with CFP-rGAT1-Δ27 and YFP-Sec24D (Fig. 10*D*). Thus, the comparison of the three different lengths of the carboxyl terminus (full length, Δ37, and Δ27) highlights the importance of the 10 amino acids between position −37 and −27 for export from the endoplasmic reticulum via the COPII-dependent machinery.

The Terminal Three Amino Acids Confer Sensitivity of GAT1 Membrane Insertion to the Exocyst—It has recently been shown that the exocyst complex is required for the regulated insertion into the plasma membrane of proteins such as the glucose transporter GLUT4 (21) and the *N*-methyl-D-aspartate receptor (21); insertion can be disrupted by dominant negative versions of Exo70. We used Exo70-GFP where the GFP moiety is fused to the carboxyl terminus of Exo70. When expressed in PC12 cells, this protein blocked differentiation (not shown) in a manner consistent with a dominant negative effect on exocyst function (23). We surmised that the reduced membrane expression of GAT1-Δ3 was due to a defect in recruiting the exocyst complex. Conversely, if membrane expression of GAT1 depended on the exocyst, coexpression of Exo70-GFP ought to decrease surface expression of the transporter. Thus, we transiently expressed wild type rGAT1 in HEK293 cells in the absence and presence of increasing amounts of Exo70-GFP. Cell surface expression was quantified by measuring cellular uptake of [^{3}H]GABA. Co-transfection with the plasmid encoding Exo70-GFP reduced [^{3}H]GABA uptake by the wild type transporter (Fig. 11). In contrast, in HEK293 cells transfected with rGAT1-Δ3, coexpression of Exo70-GFP did not cause any appreciable reduction in [^{3}H]GABA uptake (Fig. 11). A similar result was obtained using a different Exo70 construct that has been shown previously to exert a dominant negative effect on surface expression of GLUT4 (21) (Fig. 11).

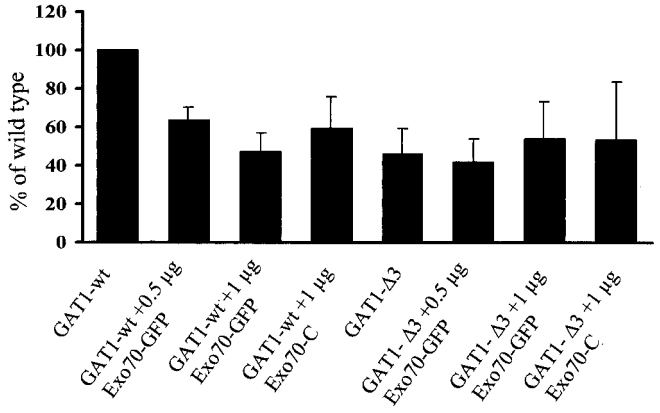

FIG. 11. **The last three amino acids confer sensitivity of rGAT1 surface expression to the exocyst.** HEK93 cells were transiently transfected with plasmids encoding YFP-rGAT1-wt and CFP-rGAT1-Δ3 alone or together with 0.5 and 1 μg of Exo70-GFP or 1 μg of Exo70-C as indicated. Uptake of [^{3}H]GABA (10 μM total GABA concentration) was determined as outlined under "Experimental Procedures." To normalize for interassay differences in transient transfections, [^{3}H]GABA uptake by cells that expressed solely the wild type transporter was used as a reference and set as 100%. This value amounted to 307 ± 124 pmol·min^{-1}·10^{-6} cells. Results are means ± S.E. (n = 3).

DISCUSSION

In the current work, we show that the carboxyl terminus of GAT1, in particular the last 28 amino acids, are crucial for expression of GAT1 at the cell surface. Our data unequivocally demonstrate the following. (i) The carboxyl terminus contains two short sequence elements (^{569}VMI^{571} and the carboxyl-terminal AYI) that are required for cell surface expression. (ii) These act in a hierarchical manner; that is the segment ^{569}VMI^{571} exerts its effects upstream of the AYI motif. This conclusion is based on the observation that the AYI motif did not rescue a GAT1 mutant that lacked the ^{569}VMI^{571} segment or in which it had been substituted by three serines. It is further supported by the observation that the two segments serve different roles during the process of sorting and delivery. The proximal segment supports the interaction with Sec24D and is thus required in the initial steps that lead to assembly of COPII vesicles. The carboxyl-terminal three amino acids are required for a later step; in their absence membrane delivery is insensitive to blockage of the exocyst. (iii) While these two segments are required for export from the endoplasmic reticulum, they do not suffice when presented solely in the context of a monomeric transporter. This conclusion is based on the observation that transporters that are deficient in oligomerization are also retained in the ER, although they are capable of recruiting Sec24 family members. In addition, the truncated version of GAT1 exerted a dominant negative effect on surface expression of wild type GAT1. This observation can also be accounted for by postulating that ER export is contingent on more than one docking site for the COPII machinery in a transporter oligomer.

It is evident that our observations are somewhat difficult to reconcile with results published earlier (7). This earlier work concluded that the last 36 amino acids of GAT1 carboxyl terminus are not relevant for membrane sorting in the polarized epithelial cell line MDCK. We are at a loss to resolve the discrepancy between our observations and those of Perego *et al.* (7). We stress that we also introduced precisely the same mutation studied by Perego and coworkers (that is GAT1-Δ36), and we also used three polarized cell types, namely the renal MDCK cell line, differentiated PC12 cell line, and most importantly hippocampal neurons. We consider the observations with the PC12 cells as well as with the neurons of particular relevance because neurotransmitter transporters are obviously enriched in the presynaptic specialization and thus targeted to the axonal compartment. In contrast, sorting in epithelial cells may be less conclusive because it relies on an extrapolation from the approximative rule that apical sorting in polarized epithelial cells predicts axonal targeting in neuronal cells. In fact, there is precedence for transmembrane proteins that do not conform to this rule (24, 25). Finally we do not consider that our analysis is confounded by the presence of a fluorescent tag at the amino terminus of GAT1 because YFP-GAT1 was delivered to the correct membrane compartment, that is the plasma membrane of the neurite extension of differentiated PC12 cells as well as to the axonal compartment of hippocampal neurons. The amino terminus of GAT1 is the site of the interaction with syntaxin 1A (26). This interaction is subject to regulation by protein kinase C, and this is thought to underlie the ability of protein kinase C to drive endocytosis and recycling of GAT1 (27). However, the amino-terminal YFP does not interfere with protein kinase C-induced removal of GAT1 from the cell surface: following transient activation of protein kinase C, unmodified GAT1 and GAT1 that carries YFP on its amino terminus undergo internalization and recycling with comparable kinetics (6). Recently Chiu *et al.* (13) reported in a mouse knock-in model that the murine GAT1, when tagged on its amino terminus with GFP, was retained within the cell. However, we observed that amino-terminally tagged rat GAT1 was efficiently delivered to the cell surface and to the axonal compartment of rat hippocampal neurons. While we cannot and do not formally rule out a rule of the amino terminus of GAT1 in sorting and membrane targeting, our data clearly identify a prominent contribution of the carboxyl terminus. We are at a loss to explain this discrepancy by any means other than to invoke a difference between murine and rat GAT1.

PDZ domains function as protein-protein interaction modules. Originally they were found to mediate interaction with specific carboxyl-terminal motifs (28); more recently, however, interactions with non-terminal motifs have also been documented (29). The PDZ-binding motif is composed of three amino acids. Interaction with class I PDZ domains requires the presence of a hydroxy group at the −2 position (serine or threonine) (29). For interaction with class II PDZ domains a hydrophobic or non-polar amino acid at −2 is required (30). In the case of GAT1, position −2 is occupied by alanine, which fulfills the criterion of a non-polar residue. This suggests that GAT1 carboxyl terminus interacts with a class II PDZ domain-containing protein. When used as a prey in a yeast two-hybrid interaction hunt, the carboxyl terminus of GAT1 interacted with Pals-1 (15). Importantly Pals-1 contains a class II PDZ domain with a high homology to CASK/Lin-2 (15). It is, however, unlikely that Pals-1 is an obligate interaction partner for GAT1. This argument is based on the fact that Pals-1 is not expressed in HEK293 cells (16); nevertheless GAT1 is efficiently inserted into the plasma membrane of these cells. Our results imply that the PDZ-binding motif is responsible for the interaction with a rate-limiting factor rather than being responsible for targeting and sorting the protein to the plasma membrane compartment. This interpretation is supported by the following findings. (i) GAT1 in which the PDZ interaction motif was deleted or mutated was targeted to the plasma membrane of HEK293 cells, but surface expression was significantly lesser than in wild type GAT1. (ii) The mutant GAT1 in which the PDZ-binding motif was ablated was still enriched in the growth cone and at the sites of sprouting neurites in differentiated PC12 cells in a manner similar to the wild type protein. Thus targeting was not impaired, although a significant portion of the mutant was detected intracellularly. (iii) Fusing the

AYI motif to GAT1-Δ37 did not rescue the protein from intracellular retention. Taken together these data show that the proximal portion of the carboxyl terminus suffices to specify delivery of GAT1 to the correct membrane compartment. The PDZ interaction domain at the carboxyl terminus confers exocyst sensitivity to GAT1.

The docking of exocytic vesicles to the plasma membrane in eukaryotic cells is mediated by a multiprotein complex known as the exocyst. The exocyst is composed of eight proteins: Sec3p/5p/6p/8p/10p/15p, Exo70, and Exo84. The exocyst proteins localize to areas of active cell surface expansion including sprouting neurites and axonal synapses (31). Recently Exo70 was also shown to mediate the regulated insertion of GLUT4 into the plasma membrane (21). Here we clearly demonstrate that surface expression of GAT1 is also dependent on Exo70 and thus on the exocyst. An analogous finding was reported for the *N*-methyl-D-aspartate receptor subunit NR2 (22): surface expression of NR2 was reduced by coexpression of a dominant negative version of Sec8p (Sec8p-Δ4). Interestingly we observed that rGAT1-Δ3 was completely insensitive to Exo70-GFP as well as to the previously described dominant negative Exo70-C. Again there is striking analogy with NR2: removal of the last seven amino acids from NR2 renders the resulting mutant insensitive to the dominant negative action of Sec8-Δ4 (22). This observation led Sans *et al.* (22) to postulate the existence of a default, exocyst-independent pathway for delivery of receptor subunits to the plasma membrane. We speculate that the same holds true for the GABA transporter and that this pathway allows GAT1-Δ27 and the mutants truncated up to position −3 to reach the plasma membrane albeit less efficiently.

Plasma membrane proteins are subject to quality control in intracellular compartments, in particular in the ER and the Golgi: if they fail to pass, they are retained. We have previously shown that GAT1 assembles into homo-oligomeric complexes and that this is an early event in biogenesis because it can be observed during ongoing synthesis in the ER (6). If the oligomerization is disrupted by point mutations, the monomeric version of GAT1 is retained in the endoplasmic reticulum, although it is not misfolded. Thus, because it is a prerequisite for ER export, oligomer formation presumably serves as an element of ER proofreading (that goes beyond the normal ER quality control system for misfolded proteins); similar conclusions have also been reached by Torres *et al.* (11) for the dopamine transporter. The present observations confirm and extend the model. The truncated versions of GAT1 that were retained were not misfolded (provided that they were assayed in vesicular preparations, they translocated substrate in a manner indistinguishable from the wild type); in addition, they also formed oligomers with the wild type protein. This was confirmed by three independent methods of FRET microscopy. This complex formation resulted in intracellular retention of wild type GAT1. Originally proteins were thought to be retained based on the exposure of ER retention signals (*e.g.* R*X*R). During protein synthesis and maturation, these signals become masked, allowing proteins to escape to the Golgi and ultimately to the plasma membrane. However, in recent years it has increasingly been appreciated that exit from the ER is an active process that depends on signals in the protein. Examples include diacidic and dihydrophobic motifs. The diacidic motif (DIE) of the vesicular stomatitis virus glycoprotein (32) has been shown to accelerate the rate of ER export. Kir2.1 potassium channels also contain a functionally relevant diacidic motif (underlined) in the sequence FCYENE; mutation of this signal leads to intracellular retention of the protein (33). Dihydrophobic motifs are usually found at the extreme end of the carboxyl terminus (*e.g.* ERGIC-53, Ref. 34). There is, however, precedence for the presence dihydrophobic signals within the polypeptide chain (*e.g.* in Erv41p and Erv46p, Ref. 35). It is tempting to speculate that, in the carboxyl terminus of GAT1, the ^{569}VMI^{571} sequence may represents an ER export motif. Mutation of all three hydrophobic residues to serine led to complete retention of the transporter in the ER. Mutation of any of the hydrophobic residues to serine affected surface expression, but the mutants were still sensitive to the exocyst.[2] Thus, the presence of all three hydrophobic residues is crucial for ER export. Importantly vesicular stomatitis virus glycoprotein forms oligomers. If the export signal of vesicular stomatitis virus glycoprotein is mutated, the protein is still capable of assembling into a homotrimer, but export of the protein to the cell surface is disrupted (32). There is a self-evident analogy between these observations and our results with mutated versions of GAT1. In view of this similarity, we propose that a single export motif, provided by one monomer, does not suffice to mediate ER export. This hypothesis is supported by the distinct abilities of various GAT1 mutants to interact with Sec24D. The rationale for choosing a Sec24 representative is as follows: Sec24 proteins are members the COPII. COPII vesicles are composed of the Sar1 GTPase, Sec23p-Sec24p complex, and Sec13p-Sec31p complex. Cargo molecules present different signals that are deciphered by the COPII components, and Sec24 members are the prime candidate for mediating initial cargo recognition (36, 37); in fact, yeast Sec24p contains a minimum of three distinct binding regions (19, 20). We used FRET microscopy because it allowed the visualization of the interaction between Sec24D and GAT1 mutants within living cells. The results obtained further supported our hypothesis that ER export is contingent upon oligomerization. (i) The mutant rGAT1-L97A,L104A is indistinguishable from the wild type transporter if activity is assessed in vesicles (6); thus it is not misfolded. Nevertheless it is not expressed at the cell surface but rather retained in the ER, and this may be related to its inability to form oligomers (6). Sec24D interacted with rGAT1-L97A,L104A, which does not suffice to support ER export. (ii) Sec24D did not bind to CFP-rGAT1-Δ37. This mutant was not deficient in oligomerization (see Figs. 2 and 3), but it lacked the export signal. (iii) Overexpression of CFP-rGAT1-Δ37 retained the wild type transporter in the cell. Thus, in the resulting mixed oligomers, the signal provided by wild type rGAT1 became limiting; in other words, a single signal does not suffice to support ER export. We therefore propose that oligomerization serves to bring export signals together to ensure efficient export of the protein from intracellular compartments.

REFERENCES

1. Rudnick, G., and Clark, J. (1993) *Biochim. Biophys. Acta* **1144,** 249–263
2. Iversen, L. (2000) *Mol. Psychiatry* **5,** 357–362
3. Blakely, R. D., Ramamoorthy, S., Schroeter, S., Qian, Y., Apparsundaram, S., Galli, A., and DeFelice, L. J. (1998) *Biol. Psychiatry* **44,** 169–178
4. Kostova, Z., and Wolf, D. H. (2003) *EMBO J.* **22,** 2309–2317
5. Schmid, J. A., Scholze, P., Kudlacek, O., Freissmuth, M., Singer, E. A., and Sitte, H. H. (2001) *J. Biol. Chem.* **276,** 3805–3810
6. Scholze, P., Freissmuth, M., and Sitte, H. H. (2002) *J. Biol. Chem.* **277,** 43682–43690
7. Perego, C., Bulbarelli, A., Longhi, R., Caimi, M., Villa, A., Caplan, M. J., and Pietrini, G. (1997) *J. Biol. Chem.* **272,** 6548–6592
8. Boehm, S., and Betz, H. (1997) *J. Neurosci.* **17,** 4066–4075
9. Miyawaki, A., and Tsien, R. Y. (2000) *Methods Enzymol.* **327,** 472–500
10. Youvan, D. C., Coleman, W. J., Silva, C. M., Petersen, J., Bylina, J., and Yang, M. M. (1997) *Biotechnol. et alia* **1,** 1–16
11. Torres, G. E., Carneiro, A., Seamans, K., Fiorentini, C., Sweeney, A., Yao, W. D., and Caron, M. G. (2003) *J. Biol. Chem.* **278,** 2731–2739
12. Radian, R., Ottersen, O. P., Storm-Mathisen, J., Castel, M., and Kanner, B. I. (1990) *J. Neurosci.* **4,** 1319–1330
13. Chiu, C. S., Jensen, K., Sokolova, I., Wang, D., Li, M., Deshpande, P., Davidson, N., Mody, I., Quick, M. W., Quake, S. R., and Lester, H. A. (2002) *J. Neurosci.* **22,** 10251–10266
14. Kappeler, F., Klopfenstein, D. R., Foguet, M., Paccaud, J. P., and Hauri, H. P.

[2] V. Paulitsche, M. Freissmuth, and H. Farhan, unpublished results.

(1997) *J. Biol. Chem.* **272,** 31801–31808
15. McHugh, E. M., Zhu, W., and Mager, S. (2001) *Soc. Neurosci. Abstr.* **27,** 242
16. Kamberov, E., Makarova, O., Roh, M., Liu, A., Karnak, D., Straight, S., and Margolis, B. (2000) *J. Biol. Chem.* **275,** 11425–11431
17. Niethammer, M., Valtschanoff, J. G., Kapoor, T. M., Allison, D. W., Weinberg, T. M., Craig, A. M., and Sheng, M. (1998) *Neuron* **20,** 693–707
18. Barlowe, C. (2003) *Trends Cell Biol.* **13,** 295–300
19. Miller, E. A., Beilharz, T. H., Malkus, P. N., Lee, M. C., Hamamoto, S., Orci, L., and Schekman, R. (2003) *Cell* **114,** 497–509
20. Mossessova, E., Bickford, L. C., and Goldberg, J. (2003) *Cell* **114,** 483–495
21. Inoue, M., Chang, L., Hwang, J., Chiang, S. H., and Saltiel, A. R. (2003) *Nature* **422,** 629–633
22. Sans, N., Prybylowski, K., Petralia, R. S., Chang, K., Wang, Y. X., Racca, C., Vicini, S., and Wenthold, R. J. (2003) *Nat. Cell Biol.* **5,** 520–530
23. Vega, I. E., and Hsu, S. C. (2001) *J. Neurosci.* **21,** 3839–3848
24. Gu, H. H., Ahn, J., Caplan, M. J., Blakely, R. D., Levay, A. I., and Rudnick, G. (1996) *J. Biol. Chem.* **271,** 18100–18106
25. Wozniak, M., and Limbird, L. E. (1998) *Brain Res.* **780,** 311–322
26. Quick, M. W., Corey, J. L., Davidson, N., and Lester, H. A. (1997) *J. Neurosci.* **17,** 2967–2979
27. Beckman, M. L., Bernstein, E. M., and Quick, M. W. (1998) *J. Neurosci.* **18,** 6103–6112
28. Kornau, H. C., Schenker, L. T., Kennedy, M. B., and Seeburg, P. H. (1995) *Science* **269,** 1737–1740
29. Xu, X. Z., Choudhury, A., Li, X., and Montell, C. (1998) *J. Cell Biol.* **142,** 545–555
30. Harris, B. Z., and Lim, W. A. (2001) *J. Cell Sci.* **114,** 3219–3231
31. Hazuka, C. D., Foletti, D. L., Hsu, S. C., Kee, Y., Hopf, F. W., and Scheller, R. H. (1999) *J. Neurosci.* **19,** 1324–1334
32. Nishimura, N., and Balch, W. E. (1997) *Science* **277,** 556–558
33. Ma, D., Zerangue, N., Lin, Y. F., Collins, A., Yu, M., Jan, Y. N., and Jan, L. Y. (2001) *Science* **291,** 316–319
34. Nufer, O., Guldbransen, S., Degen, M., Kappeler, F., Paccaud, J. P., Tani, K., and Hauri, H. P. (2002) *J. Cell Sci.* **115,** 619–628
35. Otte, S., Belden, W. J., Heidtman, M., Liu, J., Jensen, O. N., and Barlowe, C. (2001) *J. Cell Biol.* **152,** 503–518
36. Peng, R., Grabowski, R., De Antoni, A., and Gallwitz, D. (1999) *Proc. Natl. Acad. Sci. U. S. A.* **96,** 3751–3756
37. Springer, S., and Schekman, R. (1998) *Science* **281,** 698–700